



Published in final edited form as:

Oncogene. 2019 November ; 38(48): 7329–7341. doi:10.1038/s41388-019-0945-9.

MAPKAPK2 (MK2) inhibition mediates radiation-induced inflammatory cytokine production and tumor growth in head and neck squamous cell carcinoma

Kiersten L. Berggren^{1,2}, Sebastian Restrepo Cruz^{1,2}, Michael D Hixon^{1,2}, Andrew Cowan^{3,4}, Stephen B. Keysar⁵, Stephanie Craig⁶, Jacqueline James⁶, Marc Barry⁷, Michelle A. Ozbun^{4,8}, Antonio Jimeno⁵, Dennis J. McCance⁷, Ellen J. Beswick⁹, Gregory N. Gan¹⁰

¹The University of New Mexico, Department of Internal Medicine, Section of Radiation Oncology, Albuquerque, NM

²The University of New Mexico Comprehensive Cancer Center, Cancer Therapeutics Program, Albuquerque, NM

³The University of New Mexico, Department of Surgery, Division of Otolaryngology, Albuquerque, NM

⁴The University of New Mexico Comprehensive Cancer Center, Cancer Biology and Signaling Program, Albuquerque, NM

⁵University of Colorado Denver, Department of Medicine, Division of Medical Oncology

⁶Center for Cancer Research and Cell Biology, Queen's University, Belfast BT9 7BL, Northern Ireland, UK

⁷The University of New Mexico, Department of Pathology, Albuquerque, NM

⁸The University of New Mexico, Department of Molecular Genetics and Microbiology, Albuquerque, NM

⁹University of Utah, Department of Internal Medicine, Division of Gastroenterology, Hepatology, and Nutrition, Salt Lake City, UT

¹⁰University of Kansas, School of Medicine, Department of Radiation Oncology, Kansas City, KS

Abstract

Radiation therapy (RT) is a cornerstone of treatment in the management of head and neck squamous cell carcinomas (HNSCC), yet treatment failure and disease recurrence are common. The p38/MK2 pathway is activated in response to cellular stressors, including radiation, and promotes tumor inflammation in a variety of cancers. We investigated MK2 pathway activation in

Users may view, print, copy, and download text and data-mine the content in such documents, for the purposes of academic research, subject always to the full Conditions of use:http://www.nature.com/authors/editorial_policies/license.html#terms

Corresponding author: Gregory N. Gan, 4001 Rainbow Blvd, MS 4033, Kansas City, KS 66160. (913)588-3612, greg.gan@gmail.com.

Supplementary information is available at *Oncogene's* website.

The authors declare no potential conflicts of interest.

HNSCC and the interaction of MK2 and RT *in vitro* and *in vivo*. We used a combination of an oropharyngeal SCC tissue microarray, HNSCC cell lines and patient-derived xenograft (PDX) tumor models to study the effect of RT on MK2 pathway activation and to determine how inhibition of MK2 by pharmacologic (PF-3644022) and genetic (siRNA) methods impacts tumor growth. We show that high phosphorylated MK2 (p-MK2) levels are associated with worsened disease specific survival in p16-negative HNSCC patients. RT increased p-MK2 in both p16-positive, HPV-positive and p16-negative, HPV-negative HNSCC cell lines. Pharmacologic inhibition or gene silencing of MK2 *in vitro* abrogated RT-induced increases in p-MK2; inflammatory cytokine expression and expression of the downstream MK2 target, heat shock protein 27 (HSP27); and markers of epithelial-to-mesenchymal transition. Mouse PDX models treated with a combination of RT and MK2 inhibitor experienced decreased tumor growth and increased survival. Our results suggest that MK2 is a potential prognostic biomarker for head and neck cancer and that MK2 pathway activation can mediate radiation resistance in HNSCC.

Introduction

Head and neck cancers account for approximately 60,000 new cancer cases, and 12,000 deaths in the United States each year [1]. Human papillomavirus (HPV) is responsible for an increasing proportion of head and neck oropharyngeal squamous cell carcinomas (HNSCC). Compared to HPV-negative (HPV-) HNSCC, HPV+ cancers respond better to treatment, yet overall survival remains dismal particularly among patients with significant smoking histories [2-4]. While radiation therapy (RT) or combined chemo-radiotherapy are mainstays in the treatment of both p16-positive (p16+) [p16 positivity is considered a surrogate for HPV positive disease [5]] and p16-negative (p16-) HNSCC, disease recurrence and treatment failure are common [6, 7]; the mechanisms of treatment resistance in both p16+ and p16- cancers have yet to be elucidated.

The p38/MAPK pathway is activated by cellular stress signals such as cytokine signaling, hypoxia, oxidative stress, and radiation [8-10]. Upon stimulation, p38 phosphorylates MAPKAPK2 (MK2), which leads to inflammatory cytokine production (e.g., TNF- α , IL-1 α , IL-1 β , IL-6), epithelial-to-mesenchymal transition (EMT), DNA damage resistance and cell proliferation [10, 11]. MK2 knockout studies *in vitro* and *in vivo* show that MK2 is required for the stability and production of TNF- α , IL-6, and IL-1 β [12, 13]. p38/MK2-induced cytokine production may function as a positive feedback mechanism to perpetuate cytokine expression.

Neutrophilia and increased neutrophil-to-lymphocyte ratios (NLR) are markers of inflammation and are shown to be associated with decreased overall survival in HNSCC [14-16]. Furthermore, high expression of downstream inflammatory cytokines is associated with worse overall survival in HNSCC [17, 18]. High serum IL-6 levels were associated with cancer recurrence and lower overall survival [17, 19], and high plasma TNF- α levels were associated with high rates of cachexia and decreased survival in HNSCC patients [18]. In oral squamous cell carcinoma, IL-1 α enhanced cancer-associated fibroblast (CAF) proliferation *in vitro*, and tumor growth *in vivo* [20]. Pharmacologically blocking IL-6 signaling led to decreased proliferation and migration *in vitro*, enhanced cisplatin and

radiation sensitivity, and decreased tumor growth *in vivo* [21]. Targeted inhibition of MK2 led to decreased cytokine production and decreased tumor volumes in different mouse models of colorectal cancer [22, 23] and high p-MK2 levels were associated with decreased survival in HNSCC [24].

In addition to inducing an increased inflammatory phenotype, MK2 signaling activates downstream target heat shock protein 27 (HSP27) [10, 25], a chaperone protein involved in cell development, cell differentiation and apoptosis. HSP27 is overexpressed in multiple cancers [26], and is associated with poor patient outcomes in lung cancer [27]. HSP27 can also mediate the effects of certain therapeutic approaches. RT increased levels of HSP27 and p-HSP27 in head and neck cancer cell lines [28], and in mouse lung *in vivo* [29]. Pavan and colleagues [30] found that HSP27 was required for spontaneous lung metastasis in a mouse model of ovarian cancer and inhibition of HSP27 has been shown to sensitize tumors to chemotherapy [30] and RT [31].

We have investigated the role of MK2 and downstream inflammatory signaling in radiation resistance in HNSCC. We show that p-MK2 is associated with worse patient outcomes in p16- disease. We also show that p-MK2 expression is increased following RT in patient-derived xenografts (PDX) in mice. Knockdown of p-MK2 by way of selective pharmacologic inhibition or siRNA abrogates RT-induced cytokine signaling and HSP27/p-HSP27 levels in both HPV+ and HPV- HNSCC cell lines. Combining RT with inhibition of p-MK2 resulted in decreased tumor volumes compared to RT alone *in vivo*. These data suggest that targeting MK2/HSP27 signaling may be a potential therapeutic option in HNSCC.

Results

p-MK2 is expressed in human HNSCC

We examined normal, non-cancerous human head and neck tissue archived at the University of New Mexico (UNM) Human Tissue Repository and Translational Analysis Shared Resource (HTR-TASR) for p-MK2 staining by immunohistochemistry (Figure 1A). p-MK2 stains in both the nucleus and cytoplasm and is consistent with other previously published work [24]. Overall, normal epithelial tissue had few p-MK2 positive cells, with staining observed predominantly in the basal and para-basal tissue layers (independently confirmed by GNG and DJM). We also observed low levels of p-MK2 in the stromal tissue. p-MK2 was readily detected in both tumor and stromal compartments in all primary human HNSCC tumor samples evaluated suggesting that MK2 pathway activation is not dependent on p16 status (Figure 1B). HALO analysis indicated that the percentage of tissue positive for p-MK2 staining was significantly higher in p16-negative HNSCC samples compared to normal tissue in both the tumor and the stroma (Supplementary Figure S1). HSP27, a downstream target of MK2, is phosphorylated by activated p-MK2. We observe a similar pattern of staining with p-HSP27 in both the human tumor tissue and in its stromal microenvironment. The cell proliferation marker, Ki67, was also highly expressed in all HNSCC tumor tissues examined suggesting high levels of tumor proliferation (Supplementary Figure S2).

High p-MK2 expression is associated with worse disease specific survival in HPV–/p16– patients

To determine if p-MK2 could prognosticate head and neck cancer outcome, we used a clinically annotated TMA with outcomes data. We then examined whether high versus low levels of p-MK2 were associated with differences in survival in p16+ and p16– cases. Overall, we observed a significant difference in disease specific survival (DSS) with patients having p16–/p-MK2 high tumors experiencing the worst outcomes. The median DSS for the p16–, high MK2 phosphorylation group was the worst compared to the p16– low MK2 phosphorylation group (18 months vs. 68 months). Conversely, p16+/p-MK2 low (or high) patients had significantly better outcomes with no appreciable difference in survival (Figure 2A). Evaluating overall survival (OS) and stratifying among these four groups revealed that overall survival (OS) was primarily driven by p16 status (Supplementary Figure S3). Figure 2B shows p-MK2 immunohistochemistry and matched quantification notations in representative samples.

RT increases p-MK2 expression in mouse PDX models of HNSCC

Since the level of p-MK2 was elevated in tumor tissue compared to normal tissue, we wanted to determine if the levels would change following RT. p16– (HN009, CUHN004) and p16+ (HN013, HN011P) PDXs, were treated with or without RT (5Gy x2, spaced 7 days apart) (Figure 3A). Forty-eight hours after the last dose of RT, mice were sacrificed, and tumors harvested and processed for p-MK2 immunohistochemistry. Similar to the primary human tumors from which the PDXs were derived, p-MK2 was present in both tumor and stromal compartments (Figure 3B). HALO quantification showed that tumoral p-MK2 expression was increased in RT-treated mice compared to control mice in both p16– and p16+ PDXs (Figure 3B). These findings suggest RT-induced MK2 pathway activation regardless of p16 status.

Dual RT and MK2i treatment abrogates RT-induced p-MK2, p-HSP27, inflammatory cytokine, and EMT gene upregulation

We wanted to determine if RT could induce inflammatory cytokines production and activate EMT, and whether p-MK2 was important for cytokine induction. TU167 (HPV–) and SCC47 (HPV+) cell lines were treated with sham therapy, RT alone, MK2i alone, or with RT +MK2i. Cells were harvested 48 hours after treatment and RT-qPCR and immunoblots were performed. By immunoblot, RT increased MK2 protein phosphorylation while MK2 inhibitor alone did the opposite. Dual RT+MK2i treatment prevented RT-induced MK2 phosphorylation in both cell lines (Figure 4A). Because RT and MK2i can affect MK2 phosphorylation, we wanted to examine whether the downstream effector pathways (inflammation and EMT) would be affected. RT alone resulted in significant upregulation of the tumor inflammatory cytokine mRNAs in both the HPV– and HPV+ cell lines (Figure 4B). Dual RT+MK2i treatment suppressed the RT-induced increases in IL-1 α , IL-1 β , and IL-6 mRNA levels. The EMT genes SNAI1, SNAI2 and vimentin (VIM) exhibited a similar response with an increase in RT-mediated EMT gene expression and persistent suppression of these genes with dual RT+MK2i treatment (Figure 4C). In order to confirm the replicability of these findings in relation to HPV– disease, this experiment was conducted in

duplicate in three additional HPV– cell lines (SCC25, Cal27, and FaDu) with similar results (see Supplementary Figure S4).

siRNA knockdown of MK2 decreases inflammatory cytokine gene expression in HPV+ and HPV– cell lines

We then used a genetic approach to determine whether the MK2 pathway was necessary for mediating the RT-induced inflammatory cytokine production. We used short-interfering RNAs (siRNA) to knockdown MK2 in our HNSCC cell lines and subjected scramble and MK2 knockdown cells to RT. MK2 siRNA effectively knocked down MK2 mRNA and protein expression in both cell lines tested. RT increased p-MK2, p-HSP27, and IL-6 protein expression, but MK2 siRNA abrogated these RT-induced increases in each cell line (Figure 5A). Regardless of p16/HPV status, the depletion of p-MK2 led to a reduction in the mRNA levels of IL-1 α , IL-6 and TNF- α following RT treatment (Figure 5B). These findings suggest that RT-mediated, pro-tumorigenic inflammatory cytokine production is mediated through the MK2 pathway.

Dual RT-MK2i treatment slowed tumor growth and suppressed cytokine production in vivo

To determine if inhibition of MK2 phosphorylation affected tumor growth *in vivo*, we used our PDX tumor model system. We initiated tumor cell injection experiments with 2 different PDXs (HN009LN, p16–; HN011T, p16+). Mice were treated with sham therapy (control), MK2i alone, RT alone, or dual RT+MK2i (Figure 6). In both PDX models, MK2i and RT decreased tumor growth compared to the sham treated control (Figures 6A and C). When comparing dual therapy versus RT alone, the p16– PDX (HN009LN) had a significant decrease in tumor volumes ($p=0.04$) (Figure 6A, Supplementary Figure S5). In HN011T, dual treatment resulted in significantly decreased fold change in tumor volumes, compared to RT alone (Figures 6C; see Supplementary Figure S5 for raw tumor volumes). Despite treatment, a majority of the tumors in each arm eventually regrew albeit slower in the dual treatment arm compared to the monotherapy or sham arms.

Over the course of the experiments, we observed that the rate of growth of untreated HN009LN tumors was faster compared to the HN011T tumors, and HN009LN tumors became very cystic and ulcerated and importantly, caused animals to be euthanized early. Though broad conclusions cannot be made based on single PDXs, this could reflect an important difference in tumor characteristics between p16– and p16+ that may affect how they respond to treatment. To further investigate these differences we looked at the overall animal survival due to tumor burden as a surrogate for therapeutic efficacy (or treatment toxicity). We examined animal survival based on treatment arm for both HN009LN and HN011T ($n=5-7$ animals per arm), and dual therapy resulted in the longest median overall survival benefit compared to monotherapy or sham treatment (Figures 6B and D). In both PDXs we did not observe any significant changes with animal weight to suggest treatment toxicity during the treatment phase between the 4 treatment arms (data not shown). These findings support the notion that MK2i treatment combined with RT can improve overall animal survival with the greatest observed benefit, as anticipated, being in our p16+ HN011T PDX, as patients with p16+ tumors respond better to RT than patients with p16– tumors.

Because of the response observed in our p16⁻ PDXs, we wanted to confirm whether MK2 inhibition could similarly block pro-tumorigenic inflammatory cytokine production. Supernatants from these PDX tumor tissues were used for human-specific cytokine array analysis to quantify tumor-associated cytokine levels as described previously [23]. In the HN009LN PDXs (n=5 animals per group) RT significantly increased IL-1 α and IL-6 compared to control. Dual RT+MK2i treatment significantly decreased RT-induced increases in IL-1 α , IL-1 β , and IL-6 levels, but not TNF- α levels, to sham treatment levels (Figure 7).

Discussion

Over 60% of all human malignancies are managed with RT in the definitive, neoadjuvant, adjuvant and metastatic setting for curative or palliative intent [32]. Despite the effectiveness of RT in improving loco-regional control, numerous factors contribute to disease recurrence both locally and distantly in HNSCC. We have previously shown that RT led to activation of the EMT pathway *in vitro* and that compared to monotherapy alone, the combination of RT plus EMT pathway blockade demonstrated significantly improved tumor control *in vivo* [33]. In this current work, our *in vitro* findings demonstrated that RT-induced EMT and inflammatory cytokine production is mediated through the MK2 pathway. Furthermore, our *in vivo* PDX results indicate that tumors treated with RT led to MK2 pathway activation and substantial increases in inflammatory cytokine production. MK2 pathway blockade abrogated RT-induced cytokine production and reduced *in vivo* tumor growth. Our prior work using a rectal adenocarcinoma proliferation model supports the relevance of these cytokines and their ability to rescue the growth phenotypes in cell lines wherein the MK2 pathway is inhibited [34]. The importance of the MK2 pathway on tumor proliferation and survival is likely to be broadly applicable to different tumors and tissue types.

MK2 is an important, yet understudied, downstream signaling molecule in the p38-MAPK pathway in head and neck cancer. The expression of MK2 in normal tissue is associated with tissue wound healing, fibrosis, inflammatory cytokine production, and subsequent inflammation [10, 35]. p38-MK2 pathway activation leads to tissue hyperplasia, ischemic tissue remodeling and fibrosis in a murine ischemic heart injury model. MK2 pathway blockade using either a drug or genetic approaches was able to prevent pathogenic ischemic remodeling and cardiac fibrosis [36]. However, another group found that despite the prevention of murine myofibroblast development *via* MK2 pathway inhibition, loss of MK2 led to worsening pulmonary fibrosis [37]. The function of MK2 may be tissue and (cell) compartment dependent and this is reflected in our own results (Supplemental Figure S1). MK2 phosphorylation was observed predominantly in the basal and parabasal tissue layer in our normal tonsil, tongue and larynx specimens, whereas only low levels of phosphorylated MK2 were observed in muscle and stromal compartments in these samples (Figure 1A). In contrast, in our primary head and neck cancer tissues, MK2 phosphorylation was observed at substantially higher levels in both the epithelial and stromal compartments (Figure 1B). Cytotoxic stressors such as RT can lead to an increase in MK2 phosphorylation (Figure 3) in tumor tissues, implicating the potential role of MK2 as a radiation responsive gene. We also observed that RT alone increased alpha smooth muscle actin (α SMA) in the tumor stroma, yet RT combined with MK2 inhibition led to decreased α SMA expression in the stroma (data not shown). We showed that EMT gene levels are increased with RT and abrogated

with dual RT and MK2i inhibition. These data suggest that MK2 blockade may provide resistance to EMT and/or sensitization to RT. Future evaluation of EMT-specific cell proliferation, migration and invasion will address the question of whether MK2 phosphorylation plays a role in both the tumor as well as in its respective stroma.

It is unknown whether MK2 pathway activation is associated with patient outcomes. Head and neck cancer patients with p16- or p16+ disease plus a heavy smoking history, experience worse disease-specific and overall survival rates compared to their non-smoker p16+ cohort [38]. Thus, it is possible that activation of tumor-mediated inflammation within the microenvironment may contribute to these survival discrepancies, and that MK2 pathway may mediate this inflammation and subsequent tumor growth. IL-1 β , IL-6, and TNF- α are downstream cytokines activated by MK2 [12, 13] and have been shown to induce both colorectal cancer cell [23] and head and neck cancer proliferation (data not shown). Furthermore, these tumor inflammatory cytokines have been linked with worsened patient disease-specific survival and increased rates of metastases [17, 39, 40]. A recent study has demonstrated that high total cytoplasmic MK2 protein (non-phosphorylated) was associated with worse overall survival in esophageal cancer [41]. Our TMA findings demonstrated that patients with locally-advanced HPV- oropharyngeal HNSCC with high nuclear MK2 phosphorylation had worse disease-specific survival compared to MK2 phosphorylation low patients (Figure 2). In a small head and neck cancer patient cohort, Seiwart *et al.* demonstrated that high levels of nuclear MK2 phosphorylation were associated with worse overall survival but did not report on disease-specific survival [24]. We did not see a significant difference in overall survival with our TMA dataset. This discrepancy could be due to multiple reasons, including our data having a three-fold larger sample set, that our patient dataset predominantly received surgical management upfront (78.4%) compared to chemoradiotherapy, and/or that our TMA contained exclusively oropharyngeal SCC. An additional strength of our analysis was that after initial pathologist-blinded input regarding staining intensity and tumor *versus* stromal location of p-MK2 staining, the automated HALO quantification system objectively scored all samples. Finally, the median disease specific survival for the p16-, high p-MK2 group was the worst compared to the p16- low p-MK2 group, suggesting that MK2 is a protein target of clinical interest and may prognosticate patient outcome, particularly in p16- disease.

Our *in vivo* results demonstrate greater responsiveness to MK2 inhibition in the p16- PDX compared to the p16+ PDX. In contrast to HPV/p16- cancers, HPV/p16-associated head and neck cancers generally lack mutation of the tumor suppressor gene p53 [42]. There is evidence that knockout of MK2 in p53 mutated tumors, but not in p53 wild-type tumors, results in greater chemosensitivity [43]. Our p16- PDX may therefore have been more responsive to therapy presuming mutations in p53 are commonly observed in HPV/p16- HNSCC.

Downstream cytokines regulated by MK2 include IL-1, IL-6 and TNF- α and high levels of these cytokines have been linked with worse patient outcome [17, 18]. High cytokine levels contribute significantly to cancer proliferation, treatment resistance and metastasis [19, 21, 44]. In head and neck cancer, high serum IL-6 levels are associated with cancer recurrence and lower overall survival [19]. Pharmacologically blocking IL-6 signaling led to decreased

proliferation and migration *in vitro*, and enhanced cisplatin and radiation sensitivity, and decreased tumor growth *in vivo* [21]. Conceivably these cytokines individually or in combination can affect numerous tumor and microenvironmental processes either in response to cytotoxic stress or as part of oncogenesis. Blocking MK2 expression, and, therefore downstream cytokine activity should be investigated as a potential treatment option.

There is evidence that HSP27, a downstream target of MK2, induces cytokine-mediated activation of the NF- κ B pathway [45]. These data are supported by a pulmonary inflammation model wherein MK2 knockout mice had significantly lower levels of TNF- α and decreased phosphorylated HSP27 (p-HSP27) and NF- κ B pathway signaling [46]. Additionally, Zheng and colleagues [47] showed increased HSP27 and IL-6 in chemoresistant squamous tongue carcinoma cells. This increased HSP27 expression activated NF- κ B signaling, and led to increased tumor growth *in vivo*, and high HSP27 levels were correlated with worse overall survival in human patients [47]. In glioblastoma, high levels of IL-6 can act as an autocrine-paracrine factor capable of driving tumor EMT leading to cancer cell stemness and microenvironmental changes favoring immune suppression [48]. High levels of IL-6 in these glioblastoma patients are strongly correlated with worse overall and progression-free survival [49]. We have shown that MK2 inhibition by siRNA abrogates RT-induced increases in p-HSP27 and IL-6 *in vitro* (Figures 5a). Furthermore, we have demonstrated that RT increased IL-1 α , and IL-6 *in vivo* and that MK2 pathway blockade can largely reverse and/or suppress tumor inflammatory cytokine production (Figure 7). Finally, suppression of MK2 pathway following RT significantly delayed *in vivo* tumor re-growth compared to either RT or MK2 inhibitor alone (Figure 6A). To the best of our knowledge, this is the first report of RT directly activating the MK2 pathway and use of either MK2 inhibitor or gene suppression to block radiation-mediated MK2 pathway activation in head and neck cancer. It is likely that MK2-mediated radiation sensitivity is the result of crosstalk among multiple pathways, and further investigation of the precise mechanisms responsible merit further investigation. Given the use of RT in numerous human oncologic conditions, additional studies will be needed to correlate our findings with other tumor types.

Materials and Methods

Human primary tumor tissue samples

All human tumor tissue samples were obtained in accordance with the UNM Institutional Review Board (IRB) and generation of PDXs were established under the IRB-approved protocol INST 1310. All patients provided informed consent prior to tissue submission. Normal tissues and HNSCC human tumor tissues were collected during surgery as part of the HTR-TASR program. Normal head and neck tissues (anterior tongue, larynx, tonsil, and base of tongue) were formalin fixed and paraffin-embedded using standard laboratory procedures. Tumor tissues were derived from the oral cavity, oropharynx, and larynx. UNM specific PDX tumors were generated and propagated using an adapted protocol [50-52]. A portion of fresh tumor tissue was taken at the time of surgery, formalin-fixed and paraffin-embedded for immunohistochemistry. A second portion of tissue was placed in

DMEM/FBS/pen-strep media on ice, immediately processed and implanted into the bilateral flanks of female (~6 weeks) athymic nude mice (Fox n1 nu/nu). Subsequent PDX tumors were then continually passaged in athymic nude mice. Additional primary tumor samples were obtained from an IRB approved University of Colorado protocol and gifted to us in this joint collaborative project (Jimeno Lab). Refer to Supplementary Table S1 for patient characteristics of tissues used for PDX generation and experimentation.

Human primary tissue microarray

In collaboration with Queen's University, Belfast, we examined a de-identified 180-patient oropharyngeal SCC tissue microarray (TMA) obtained from the Northern Ireland Biobank (NIB 13-001), with study approval in the United States under the UNM HRRC 15-565. Based on the UICC/AJCC 7th edition, we excluded low risk HNSCC patients who had Stage I or Stage II disease or did not receive definitive treatment. The remaining patients were defined as loco-regionally advanced (Stage III, IVA, IVB) with annotated p16 status who received definitive treatment (surgery followed by radiotherapy and/or chemotherapy or definitive radiotherapy with or without chemotherapy) leaving 111 evaluable patients. TMA slides were stained with a p-MK2 antibody (Cell Signaling Technologies, Danvers, MA) by the HTR-TASR. Stained slides were digitally scanned and acquired on an Aperio 2AT scanner. Pre-determined conditions were coded into HALO system (Indica Labs, Corrales, NM) by a blinded pathologist who helped with identifying staining intensity, percent staining of total tissue and identifying tumor cells from surrounding tissue microenvironment cells. All samples in the TMA were then subjected to machine-based image analysis. Results for nuclear staining intensity (0, 1+, 2+, 3+) and percent tumor tissue staining were obtained. Hirsch score (H-score) (intensity x percent staining) was performed for all samples. The median H-score was used as the cutoff value to classify tissue as high versus low p-MK2 staining. H-scores and p16 status were correlated and log-rank statistical analysis was performed to assess overall survival (OS) and disease-specific survival (DSS).

PDX and cell line injection experiments

All animal experiments were approved by the UNM IACUC. In the first experiment, 6-week old female athymic nude mice (Fox n1 nu/nu) with flank PDX tumors from primary base of tongue, tonsil, floor of mouth (HN011T, HN013, HN009, CUHN004) were left untreated (control), or treated with two, 5 Gy doses of RT separated by one week. UNM PDX's (HN011T, HN013, HN009) from the F2 generation or Colorado PDX (CUHN004) from the F6 generation were used for these RT-specific experiments. For the tumor volume and survival experiments, we utilized UNM PDX tumors passaged between the F4-F10 generations. Tumor tissues were harvested 48 hours after the second dose of RT and processed for immunohistochemistry or stored at -80°C for future analysis. In the second experiment, multiple tumors from each PDX (HN009LN, HN011T) were harvested, dissociated, and prepared for inoculation (1×10^6 cells/50 μ l injection volume) into new mice as previously described [33, 50, 52]. Unilateral right flank injections were administered, and tumor growth was monitored twice weekly until tumors reached approximately 100mm³ at which time animals were assigned to four groups (n = 10-12 mice/group): control, RT, MK2 inhibitor (PF-3644022, Sigma-Aldrich, St. Louis, MO) (MK2i), and RT+MK2i. For

irradiation, mice were anesthetized with a mixture of xylazine (16mg/kg) and ketamine (80mg/kg) and covered with a custom-made cerrobend shield exposing only the flank region with tumor to irradiation. Animals were exposed to a single dose of 5 Gy using a MultiRad 225 irradiator (Faxitron Bioptics LLC, Tuscon, AZ) at a rate of 2 Gy/minute, with a 225kV source, at 17.7 mA using a 0.3mm copper filter. MK2i was injected peri-tumorally (50µM, 30µl injection volume) every other day for a total of 6 injections per mouse. RT+MK2i mice were injected with MK2i four hours prior to RT. Control and RT mice received sham DMSO injections. Peritumoral injections were chosen as previously described [53]. Follow-up work in other cell lines and PDX's demonstrate similar efficacy and tumor control with intraperitoneal injections (data not shown).

Four to five mice from each group were sacrificed 48 hours after their final treatment. Tumor tissues were harvested and processed for cytokine, mRNA, and protein analysis (For HN009LN experiment: control, n=5; RT, n=6; MK2i, n=6; RT+MK2i, n=5; For HN011T experiment only 1 animal per group was used for tissue analysis). For the remainder of the study, remaining mice (for HN009LN n=5 animals/group; for HN011T control n=7; RT n=6; MK2i n=6; RT+MK2i n=7) were monitored twice weekly and tumor measurements were recorded by an unblinded technician. Mice were sacrificed promptly upon reaching a humane endpoint.

Cell culture

HNSCC cell lines were kindly gifted as follows: UM-SCC47 from Dr. Thomas Carey (University of Michigan); TU167 from Dr. Jeffrey Myers, (UT MD Anderson Cancer Center). Cell lines were verified by short tandem repeat analysis and were confirmed negative for mycoplasma infection. The p16+/HPV+ (SCC47) and p16-/HPV- (TU167) human HNSCC tumor cells were grown in DMEM (ThermoFisher, Waltham, MA) supplemented with 10% FBS and 1% penicillin-streptomycin. Cells were treated with 50µM MK2 inhibitor (PF 3644022, Tocris), RT (RT; 10Gy), both MK2i and RT, or nothing (control). Cells were irradiated using the MultiRad 225 irradiator. MK2i in low serum media (0.5% FBS) was applied to cells 4 hours prior to irradiation; immediately following RT media was exchanged for media containing 10% FBS and MK2i as previously described [33]. Cells were grown for an additional 48 hours at which time they were harvested for protein and mRNA analysis. These initial cell experiments were replicated with additional cell lines (SCC25, CAL27, FaDU) which were obtained from ATCC.

mRNA and protein analysis

RNAs were extracted and purified using the Qiagen RNeasy kit (Germantown, MD). cDNAs were produced with the Verso cDNA synthesis kit (ThermoFisher). Reverse transcription-qPCR (RT-qPCR) was performed for target genes using a C1000 Thermal Cycler (BioRad, Hercules, CA).

For protein analysis, proteins were separated using SDS-PAGE and transferred onto PVDF membranes for immunoblot. Immunoblot followed established standard techniques and the following antibodies from Cell Signaling Technologies: MK2 (#12155; clone D1E11; 1:10,000 dilution), p-MK2 (#3316; Thr222, clone 9A7; 1:1,000 dilution), HSP27 (#2402;

clone G31; 1:10,000 dilution), p-HSP27 (#9709; Ser82, clone D1H2F6; 1:2,000 dilution) were used.

Immunohistochemistry

PDX tumor samples were labeled by immunohistochemistry for p-MK2 as previously described [23]. Sections were imaged with a Zeiss AxioCamHR digital color camera mounted atop a Zeiss AxioSkop 2 MOT upright microscope (Zeiss, Oberkochen, Germany). Sections were also submitted to the UNM HTR-TASR for digitization and quantitative analysis using the HALO imaging system.

siRNA MK2 knockdown

Multiple siRNA constructs targeting MK2 were used to knockdown gene expression *in vitro* (Integrated DNA Technologies, Coralville, IA). Preliminary testing identified the construct with most efficient MK2 knockdown and experiments proceeded using this construct (see Supplementary Table S2 for construct sequences). Cell lines were plated to approximately 40% confluency in 6cm dishes and 25nM siRNA in serum-free DMEM was applied. Twenty-four hours after application of siRNA, cells were irradiated (10Gy), and media was immediately replaced with DMEM plus 10% FBS and 1% pen-strep. Cells were harvested 48 hours after irradiation and processed for mRNA and protein levels as described above.

Cytokine arrays

Representative tumor tissues from each group of animals were obtained 48 hours after the commencement of the experiment and upon reaching humane endpoint. Approximately 8mg tissue pieces were incubated in DMEM containing 10% FBS for 18 hours. Species specific (i.e. mouse, human) cytokine array analyses were performed on supernatants as described previously [23].

Statistical analysis

Statistical analyses were performed with the assistance of UNM CCC Biostatistics Core when analyzing the oropharyngeal TMA. For the TMA, specimens were sorted based on their p-MK2 staining per Hirsch index and a median distribution of 25 was established for the dataset. Samples greater than 25 were considered high p-MK2 staining while samples less than or equal to 25 were considered low p-MK2 staining. The dataset was then stratified based on their p16 status to generate 4 different groups (p16+, p-MK2 low; p16+, p-MK2 high; p16-, p-MK2 low; p16-, p-MK2 high). Log-rank analysis was performed between all four groups. Multi-variate analysis was not feasible due to small sample numbers. For *in vitro* experiments, ANOVA analysis followed by multiple comparisons (Sidak's multiple comparison test) or ANOVA analysis followed by pre-planned Student's t-test comparisons (for *in vivo* experiments)(GraphPad Prism 6) were performed for both *in vitro* and *in vivo* experiments. All *in vitro* experiments were replicated at a minimum of three separate experiments. *In vivo* animal experimental arms were statistically analyzed among groups with 5–7 animals per group. Statistical values were only shown for $p < 0.05$.

Supplementary Material

Refer to Web version on PubMed Central for supplementary material.

Acknowledgements:

Work supported in part by RSNA Foundation Research Scholar Grant, ACS-IRG (IRG-14-187-19), Dedicated Health Research Fund from the University of New Mexico School of Medicine (UNM RAC 2018), STI CRC (U19 AI 113187) and the NIH P30 Grant NCI P30CA118100. The research in this paper was supported by the Human Tissue Repository and Tissue Analysis Shared Resource, funded by the Department of Pathology and The University of New Mexico Comprehensive Cancer Center and NCI P30CA118100. Many of the images in this paper were generated in the University of New Mexico Cancer Center Fluorescence Microscopy Shared Resource with current funding from NCI 2P30 CA118100. Initial support with PDX generation was performed with the assistance from the University of New Mexico Cancer Center Animal Shared Resource funded by NCI 2P30 CA118100. We also wish to acknowledge UNM Cancer Center Biostatistics Core Facility for their statistical assistance.

References

1. Siegel RL, Miller KD, and Jemal A, Cancer statistics, 2018. *CA Cancer J Clin*, 2018 68(1): p. 7–30. [PubMed: 29313949]
2. Mirghani H, et al., Smoking impact on HPV driven head and neck cancer's oncological outcomes? *Oral Oncol*, 2018 82: p. 131–137. [PubMed: 29909887]
3. Haigentz M Jr., et al., Understanding Interactions of Smoking on Prognosis of HPV-Associated Oropharyngeal Cancers. *Adv Ther*, 2018 35(3): p. 255–260. [PubMed: 29511982]
4. Liskamp CP, et al., Adverse effect of smoking on prognosis in human papillomavirus-associated oropharyngeal carcinoma. *Head Neck*, 2016 38(12): p. 1780–1787. [PubMed: 27248701]
5. Klussmann JP, et al., Expression of p16 protein identifies a distinct entity of tonsillar carcinomas associated with human papillomavirus. *Am J Pathol*, 2003 162(3): p. 747–53. [PubMed: 12598309]
6. Argiris A, et al., Evidence-Based Treatment Options in Recurrent and/or Metastatic Squamous Cell Carcinoma of the Head and Neck. *Front Oncol*, 2017 7: p. 72. [PubMed: 28536670]
7. Argiris A, et al., Head and neck cancer. *Lancet*, 2008 371(9625): p. 1695–709. [PubMed: 18486742]
8. Munshi A and Ramesh R, Mitogen-activated protein kinases and their role in radiation response. *Genes Cancer*, 2013 4(9–10): p. 401–8. [PubMed: 24349638]
9. An SS, et al., Hypoxia alters biophysical properties of endothelial cells via p38 MAPK- and Rho kinase-dependent pathways. *Am J Physiol Cell Physiol*, 2005 289(3): p. C521–30. [PubMed: 15857906]
10. Singh RK, Najmi AK, and Dastidar SG, Biological functions and role of mitogen-activated protein kinase activated protein kinase 2 (MK2) in inflammatory diseases. *Pharmacol Rep*, 2017 69(4): p. 746–756. [PubMed: 28582691]
11. Roux PP and Blenis J, ERK and p38 MAPK-activated protein kinases: a family of protein kinases with diverse biological functions. *Microbiol Mol Biol Rev*, 2004 68(2): p. 320–44. [PubMed: 15187187]
12. Kotlyarov A, et al., MAPKAP kinase 2 is essential for LPS-induced TNF-alpha biosynthesis. *Nat Cell Biol*, 1999 1(2): p. 94–7. [PubMed: 10559880]
13. Neininger A, et al., MK2 targets AU-rich elements and regulates biosynthesis of tumor necrosis factor and interleukin-6 independently at different post-transcriptional levels. *J Biol Chem*, 2002 277(5): p. 3065–8. [PubMed: 11741878]
14. Sumner WA, et al., Survival impact of pre-treatment neutrophils on oropharyngeal and laryngeal cancer patients undergoing definitive radiotherapy. *J Transl Med*, 2017 15(1): p. 168. [PubMed: 28764811]
15. Schernberg A, et al., Prognostic factors in patients with soft palate squamous cell carcinoma. *Head Neck*, 2019.
16. Jank BJ, et al., Prognostic value of advanced lung cancer inflammation index in head and neck squamous cell carcinoma. *Eur Arch Otorhinolaryngol*, 2019.

17. Kumar B, et al., Nuclear PRMT5, cyclin D1 and IL-6 are associated with poor outcome in oropharyngeal squamous cell carcinoma patients and is inversely associated with p16-status. *Oncotarget*, 2017 8(9): p. 14847–14859. [PubMed: 28107179]
18. Powrozek T, et al., Relationship between TNF- α –1031T/C gene polymorphism, plasma level of TNF- α , and risk of cachexia in head and neck cancer patients. *J Cancer Res Clin Oncol*, 2018.
19. Duffy SA, et al., Interleukin-6 predicts recurrence and survival among head and neck cancer patients. *Cancer*, 2008 113(4): p. 750–7. [PubMed: 18536030]
20. Bae JY, et al., Reciprocal interaction between carcinoma-associated fibroblasts and squamous carcinoma cells through interleukin-1 α induces cancer progression. *Neoplasia*, 2014 16(11): p. 928–38. [PubMed: 25425967]
21. Yadav A, et al., Bazedoxifene enhances the anti-tumor effects of cisplatin and radiation treatment by blocking IL-6 signaling in head and neck cancer. *Oncotarget*, 2017 8(40): p. 66912–66924. [PubMed: 28978005]
22. Ray AL, et al., Blockade of MK2 is protective in inflammation-associated colorectal cancer development. *Int J Cancer*, 2016 138(3): p. 770–5. [PubMed: 26238259]
23. Ray AL, et al., Inhibition of MK2 suppresses IL-1 β , IL-6, and TNF- α dependent colorectal cancer growth. *Int J Cancer*, 2017.
24. Seiwert TY, et al., DNA repair biomarkers XPF and phospho-MAPKAP kinase 2 correlate with clinical outcome in advanced head and neck cancer. *PLoS One*, 2014 9(7): p. e102112. [PubMed: 25019640]
25. Stokoe D, et al., Identification of MAPKAP kinase 2 as a major enzyme responsible for the phosphorylation of the small mammalian heat shock proteins. *FEBS Lett*, 1992 313(3): p. 307–13. [PubMed: 1332886]
26. Singh MK, Sharma B, and Tiwari PK, The small heat shock protein Hsp27: Present understanding and future prospects. *J Therm Biol*, 2017 69: p. 149–154. [PubMed: 29037376]
27. Sheng B, et al., Increased HSP27 correlates with malignant biological behavior of non-small cell lung cancer and predicts patient's survival. *Sci Rep*, 2017 7(1): p. 13807. [PubMed: 29062135]
28. Muschter D, et al., A comparison of cell survival and heat shock protein expression after radiation in normal dermal fibroblasts, microvascular endothelial cells, and different head and neck squamous carcinoma cell lines. *Clin Oral Investig*, 2018 22(6): p. 2251–2262.
29. Kim JY, et al., HSP27 inhibitor attenuates radiation-induced pulmonary inflammation. *Sci Rep*, 2018 8(1): p. 4189. [PubMed: 29520071]
30. Pavan S, et al., HSP27 is required for invasion and metastasis triggered by hepatocyte growth factor. *Int J Cancer*, 2014 134(6): p. 1289–99. [PubMed: 23996744]
31. Guttman DM, et al., Inhibition of Hsp27 radiosensitizes head-and-neck cancer by modulating deoxyribonucleic acid repair. *Int J Radiat Oncol Biol Phys*, 2013 87(1): p. 168–75. [PubMed: 23849696]
32. Sharma RA, et al., Clinical development of new drug-radiotherapy combinations. *Nat Rev Clin Oncol*, 2016 13(10): p. 627–42. [PubMed: 27245279]
33. Gan GN, et al., Hedgehog signaling drives radioresistance and stroma-driven tumor repopulation in head and neck squamous cancers. *Cancer Res*, 2014 74(23): p. 7024–36. [PubMed: 25297633]
34. Ray AL, et al., Inhibition of MK2 suppresses IL-1 β , IL-6, and TNF- α -dependent colorectal cancer growth. *Int J Cancer*, 2018 142(8): p. 1702–1711. [PubMed: 29197088]
35. Thiraisingam T, et al., MAPKAPK-2 signaling is critical for cutaneous wound healing. *J Invest Dermatol*, 2010 130(1): p. 278–86. [PubMed: 19609314]
36. Xu L, et al., MMI-0100 inhibits cardiac fibrosis in myocardial infarction by direct actions on cardiomyocytes and fibroblasts via MK2 inhibition. *J Mol Cell Cardiol*, 2014 77: p. 86–101. [PubMed: 25257914]
37. Liu T, et al., Lack of MK2 inhibits myofibroblast formation and exacerbates pulmonary fibrosis. *Am J Respir Cell Mol Biol*, 2007 37(5): p. 507–17. [PubMed: 17600313]
38. Tribius S, et al., HPV status in patients with head and neck of carcinoma of unknown primary site: HPV, tobacco smoking, and outcome. *Oral Oncol*, 2012 48(11): p. 1178–84. [PubMed: 22739067]

39. Leon X, et al., Expression of IL-1alpha correlates with distant metastasis in patients with head and neck squamous cell carcinoma. *Oncotarget*, 2015 6(35): p. 37398–409. [PubMed: 26460957]
40. Cheng JC, et al., High serum levels of vascular endothelial growth factor-A and transforming growth factor-beta1 before neoadjuvant chemoradiotherapy predict poor outcomes in patients with esophageal squamous cell carcinoma receiving combined modality therapy. *Ann Surg Oncol*, 2014 21(7): p. 2361–8. [PubMed: 24623035]
41. Jomrich G, et al., MK2 and ETV1 Are Prognostic Factors in Esophageal Adenocarcinomas. *J Cancer*, 2018 9(3): p. 460–468. [PubMed: 29483950]
42. Gillison ML, et al., Evidence for a causal association between human papillomavirus and a subset of head and neck cancers. *J Natl Cancer Inst*, 2000 92(9): p. 709–20. [PubMed: 10793107]
43. Morandell S, et al., A reversible gene-targeting strategy identifies synthetic lethal interactions between MK2 and p53 in the DNA damage response in vivo. *Cell Rep*, 2013 5(4): p. 868–77. [PubMed: 24239348]
44. Qin X, et al., Cancer-associated Fibroblast-derived IL-6 Promotes Head and Neck Cancer Progression via the Osteopontin-NF-kappa B Signaling Pathway. *Theranostics*, 2018 8(4): p. 921–940. [PubMed: 29463991]
45. Park KJ, Gaynor RB, and Kwak YT, Heat shock protein 27 association with the I kappa B kinase complex regulates tumor necrosis factor alpha-induced NF-kappa B activation. *J Biol Chem*, 2003 278(37): p. 35272–8. [PubMed: 12829720]
46. Gorska MM, et al., MK2 controls the level of negative feedback in the NF-kappaB pathway and is essential for vascular permeability and airway inflammation. *J Exp Med*, 2007 204(7): p. 1637–52. [PubMed: 17576778]
47. Zheng G, et al., HSP27-Mediated Extracellular and Intracellular Signaling Pathways Synergistically Confer Chemoresistance in Squamous Cell Carcinoma of Tongue. *Clin Cancer Res*, 2018 24(5): p. 1163–1175. [PubMed: 29246940]
48. Gurgis FM, et al., The p38-MK2-HuR pathway potentiates EGFRvIII-IL-1beta-driven IL-6 secretion in glioblastoma cells. *Oncogene*, 2015 34(22): p. 2934–42. [PubMed: 25088200]
49. Yeung YT, et al., p38 MAPK inhibitors attenuate pro-inflammatory cytokine production and the invasiveness of human U251 glioblastoma cells. *J Neurooncol*, 2012 109(1): p. 35–44. [PubMed: 22528800]
50. Keysar SB, et al., Hedgehog signaling alters reliance on EGF receptor signaling and mediates anti-EGFR therapeutic resistance in head and neck cancer. *Cancer Res*, 2013 73(11): p. 3381–92. [PubMed: 23576557]
51. Stein AP, et al., Xenograft assessment of predictive biomarkers for standard head and neck cancer therapies. *Cancer Med*, 2015 4(5): p. 699–712. [PubMed: 25619980]
52. Keysar SB, et al., A patient tumor transplant model of squamous cell cancer identifies PI3K inhibitors as candidate therapeutics in defined molecular bins. *Mol Oncol*, 2013 7(4): p. 776–90. [PubMed: 23607916]
53. Ray AL, et al., Inhibition of MK2 suppresses IL-1beta, IL-6, and TNF-alpha-dependent colorectal cancer growth. *Int J Cancer*, 2017.

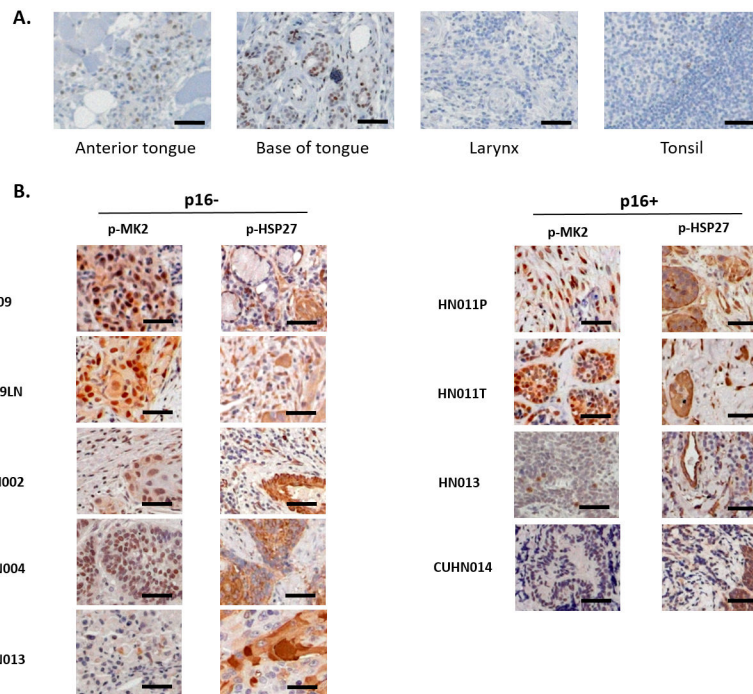


Figure 1.

Phosphorylated MK2 (p-MK2) is overexpressed in head and neck tumor tissue compared to non-cancerous human tissue. **A**, Normal human head and neck tissue was obtained from the UNM Human Tissue Repository (HTR) *via* the IRB-approved study, INST 1310 (SRC 008-17). Standard immunohistochemistry was performed on 4-micron cut tissue sections staining for p-MK2. **B**, Primary head and neck cancer tissue obtained through institutional HTR using two different IRB approved protocols (University of New Mexico: HN009, HN009LN, HN011P, HN011T, HN013; University of Colorado Denver: CUHN002, CUHN004, CUHN0013, CUHN014) were cut and stained for p-MK2. Both p16 negative (p16⁻) and p16 positive (p16⁺) primary human HNSCC tissues were examined. Black bar denotes 50 μm size.

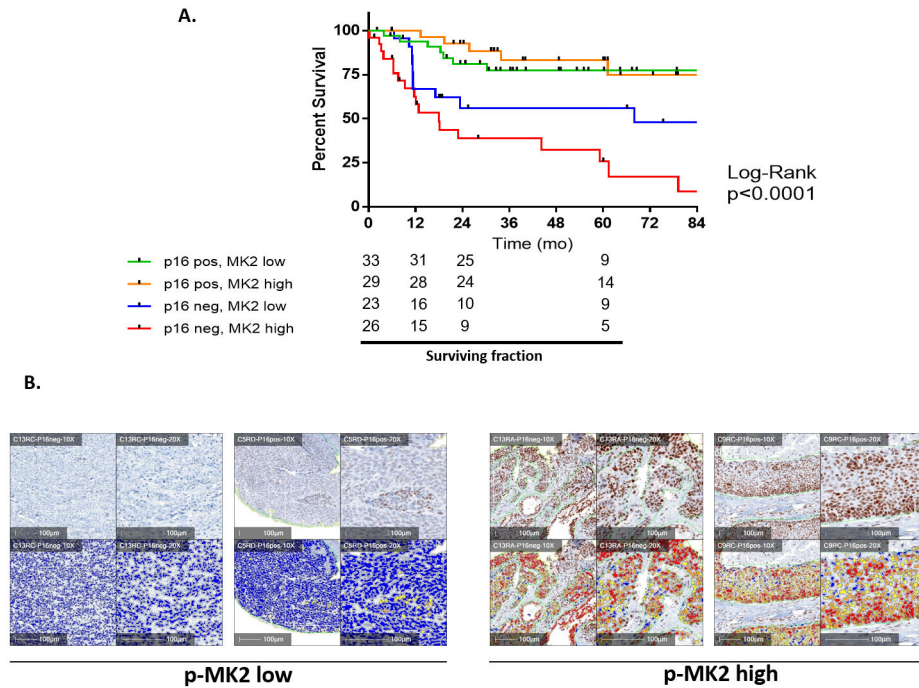


Figure 2.

High MK2 phosphorylation is a poor prognostic factor in HNSCC. **A**, Using an annotated oropharyngeal HNSCC tissue microarray, we queried whether HNSCC patients with Stage III, IV disease and high *versus* low p-MK2 levels impacted disease specific survival. Kaplan-Meier disease-specific survival curves were generated between p16+ [p-MK2 low (n = 33) *versus* MK2 high n = 29)] and p16– [p-MK2 low (n = 23) *versus* MK2 high (n = 26)] patients. Unlike the p16+ patients, the p16– patients demonstrated a significant survival difference between high versus low p-MK2 levels, p = 0.034. **B**, All tissue microarray slides were scanned at the highest digital resolution (40x) using the Aperio Imaging platform. Digitized slides were then imported into the HALO analysis system where a blinded pathologist and researcher helped to train the software program to differentiate between staining intensity (0+, 1+, 2+ and 3+) and tumor stroma versus the tumor itself. Representative p-MK2 immunohistochemistry and the respective HALO analyses was performed on p16– and p16+ samples. Representative samples here were further stratified between low versus high p-MK2 levels. Blue = 0+, yellow = 1+, orange = 2+, red = 3+. Slides were digitally rescaled from the 40x to 10x resolution. White bar denotes 100 μ m size.

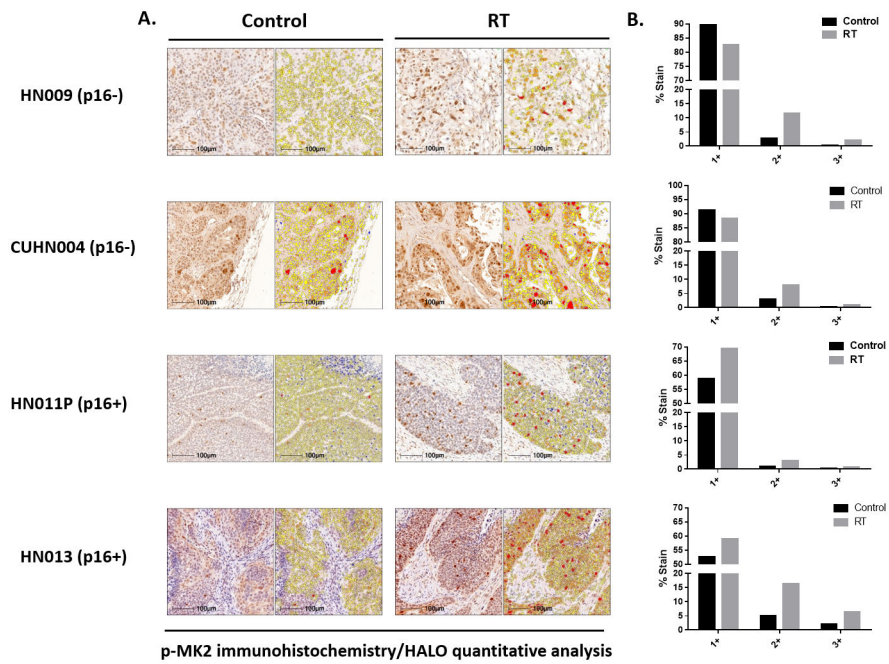


Figure 3. RT leads to MK2 phosphorylation in mouse PDXs. **A**, p-MK2 immunohistochemistry staining of various F2 generation p16⁻ and p16⁺ human PDX tumors, treated with or without RT (5Gy x 2). **B**, Quantitative HALO analyses for different representative PDX tumor samples looking at overall p-MK2 labeling between irradiated and non-irradiated samples demonstrated increased p-MK2 labeling compared to non-irradiated tissue.

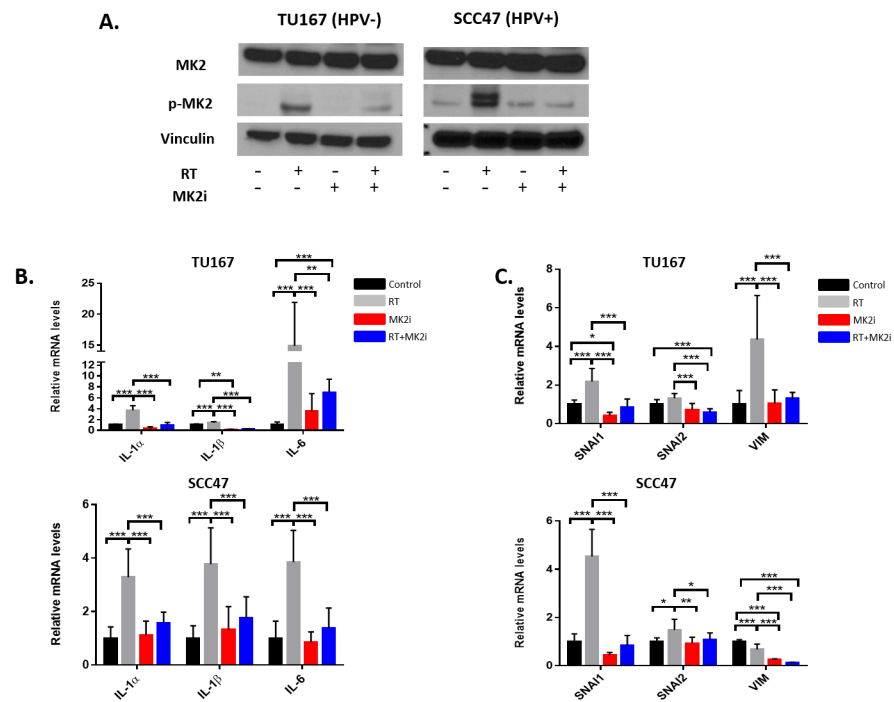


Figure 4. Protein and mRNA profiles in HPV- and HPV+ HNSCC cell lines. **A**, p-MK2 protein expression in cell lines treated with RT, MK2i, or RT+MK2i. **B**, Inflammatory cytokine gene expression in cells treated with sham, RT, MK2i or RT+MK2i in multiple tumor cell lines. **C**, EMT gene expression in cells treated with sham, RT, MK2i or RT+MK2i in multiple tumor cell lines. Significance: * = $p < 0.05$; ** = $p < 0.01$; *** = $p < 0.001$

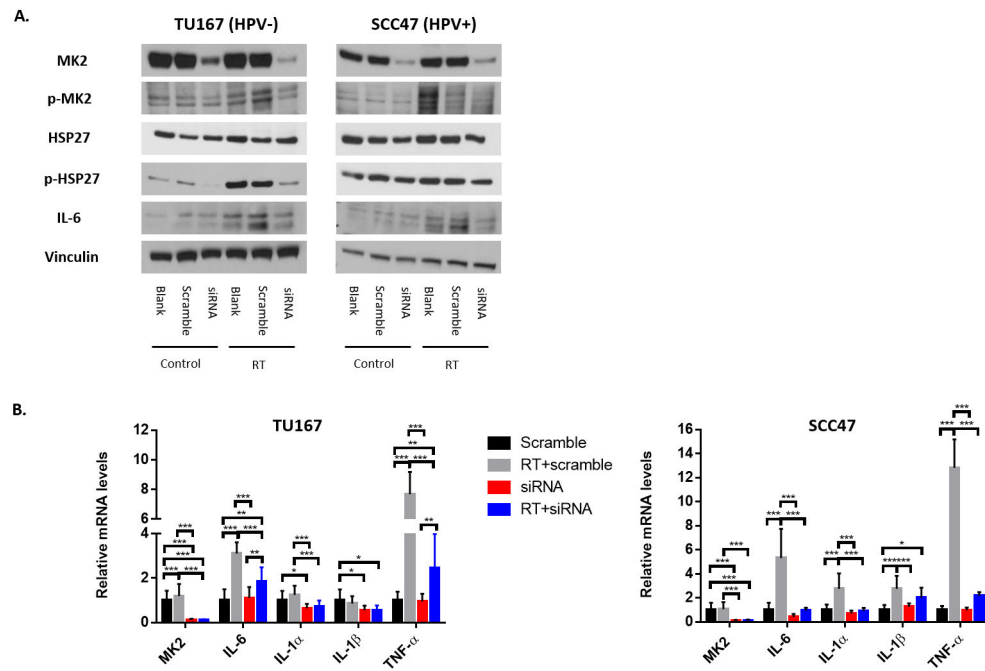


Figure 5. MK2 siRNA blocks RT-induced MK2 and HSP27 phosphorylation in HPV- and HPV+ cell lines. HNSCC cell lines were treated with siRNA, with or without RT. **A**, Protein levels of MK2, p-MK2, HSP27, p-HSP27 and IL-6 and **B**, mRNA expression for MK2, IL-6, IL-1 α , IL-1 β , TNF- α were examined. Significance: * = $p < 0.05$; ** = $p < 0.01$; *** = $p < 0.001$

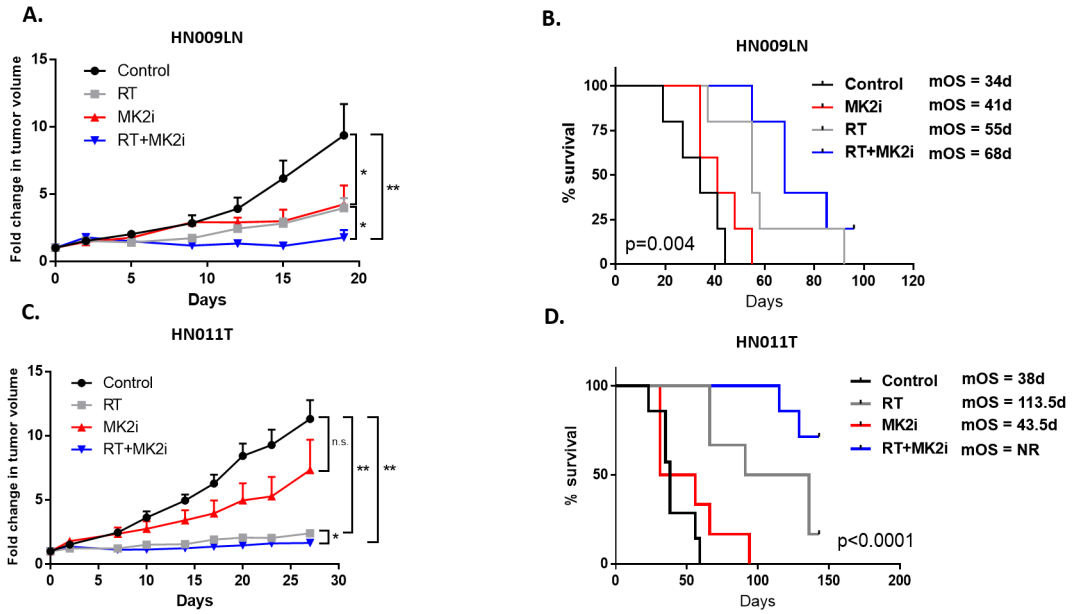


Figure 6. MK2 pathway blockade enhances RT sensitivity and blocks RT-induced pro-tumorigenic cytokine production, *in vivo*. **A and C**, Fold change in HN009LN (p16+) and HN011T (p16-) tumor volumes in mice treated with excipient, RT, MK2i, or RT+MK2i. **B and D**, PDX tumor survival curves. Athymic nude mice xenografted with HN009LN (**A**) and HN011T (**C**) tumors were monitored and euthanized appropriately per IACUC approved protocol when their tumors reached 2000 mm³, tumors became ulcerated or animals became moribund. Kaplan-Meier survival curves were generated comparing excipient/control, MK2i, RT or RT+MK2i treatment arms. Survival was measured from the first day of treatment onwards. P values noted in the survival curve (n = 5-6 animals per arm). Significance: * = p<0.05; ** = p<0.01; *** = p<0.001.

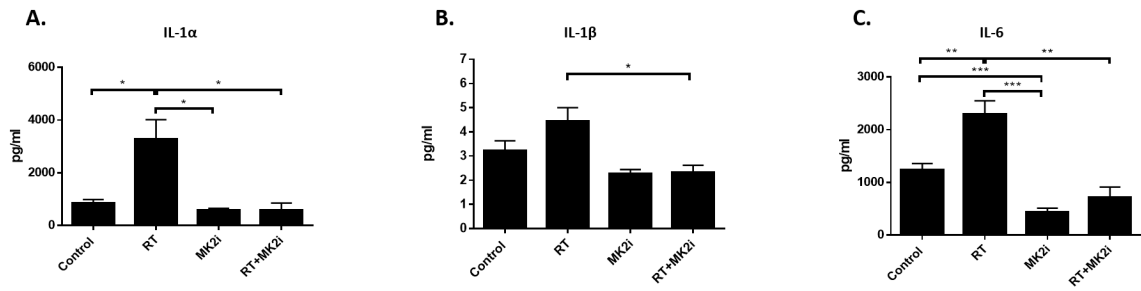


Figure 7.

In vivo tissue collection was performed 48 hours after final treatment and 8 mg of tissue was incubated in culture media for 16 hours. Human inflammatory cytokine levels from PDX tumors were analyzed using a multiplex cytokine array analyzer. **A**, IL-1 α ; **B**, IL-1 β ; **C**, IL-6. Significance: * = $p < 0.05$; ** = $p < 0.01$; *** = $p < 0.001$.